JAERI-M
84-109

CALCULATION OF ANISOTROPY CORRECTION FACTOR FOR DETERMINATION OF D-T NEUTRON YIELD BY ASSOCIATED α-PARTICLE METHOD

June 1984

Seiya YAMAGUCHI, Yukio OYAMA
and Hiroshi MAEKAWA

日本原子力研究所
Japan Atomic Energy Research Institute

JAERI-M レポートは，日本原子力研究所が不定期に公刊している研究報告書です。

入手の問合わせは，日本原子力研究所技術情報部情報資料課（〒319－11 茨城県那珂郡東海村）あて，お申しこしください。なお，このほかに財団法人原子力弘済会資料センター（〒319—11 茨城県那珂郡東海村日本原子力研究所内）で複写による実費領布をおこなっております。

JAERI-M reports are issued irregularly.

Inquiries about availability of the reports should be addressed to Information Section, Division of Technical Information, Japan Atomic Energy Research Institute, Tokai-mura, Naka-gun, Ibaraki-ken 319—11, Japan.

編集兼発行　日本原子力研究所
印　　刷　日立高速印刷株式会社

JAERI-M 84-109

Calculation of Anisotropy Correction Factor for Determination of D-T Neutron Yield by Associated α-Particle Method

Seiya YAMAGUCHI, Yukio OYAMA and Hiroshi MAEKAWA

Department of Reactor Engineering,
Tokai Research Establishment, JAERI

(Received May 24, 1984)

In the experiments at the FNS(Fusion Neutronics Source), absolute neutron yield produced by $^{3}T(d,n)^{4}He$ reaction is determined by an associated α-particle method taking the correction for anisotropy into consideration. Calculations of the anisotropy correction factor are carried out for thick-target case and its error is discussed.

The effects of following factors are examined : (1) energy loss data of deuteron in Ti-T target, (2) relativistic kinematics, (3) nonuniformity of tritium distribution in Ti-T target.

From these calculations, it is concluded that the anisotropy correction factor has uncertainty of about ± 1.5 %, of which main contribution is due to the change in tritium distribution caused by bombardment of deuteron beam.

Keywords: Fusion Neutronics, Absolute Neutron Yield, $^{3}T(d,n)^{4}He$ reaction, Associated α-particle Method, Anisotropy Correction Factor, The Rate of Energy Loss, Relativistic Kinematics, Nonuniformity of the Tritium Distribution

随伴α粒子法によるD－T中性子発生量の決定のための非等方性補正因子の計算

日本原子力研究所東海研究所原子炉工学部
山口　誠哉・大山　幸夫・前川　　洋

（1984年5月24日受理）

FNS（核融合炉物理用中性子源）における実験では，$^{3}T(d,n)^{4}He$ 反応によって生じる中性子の絶対発生量は，非等方性を考慮に入れた随伴α粒子法により決定されている。厚いターゲットに対して，非等方性補正因子の計算を行い，誤差について議論した。

ここでは，以下の項目について調べた。(1)Ti－Tターゲット中での重陽子のエネルギー損失，(2)相対論的運動学，(3)ターゲット中でのトリチウム分布の非一様性。

この計算により，非等方性補正因子は±約1.5％の不確定性を持っており，それは主として重陽子ビームの衝撃によって生じるトリチウム分布の変化によるということがわかった。

Contents

目　　次

1. Introduction

An absolute determination of the total neutron yield is essential for the estimation of tritium breeding and nuclear heating rates in the benchmark experiments on fusion reactor blanket.

At the Fusion Neutronics Source (FNS)[1,2] constructed in Japan Atomic Energy Research Institute, the absolute neutron yield produced by $^{3}T(d,n)^{4}He$ reaction is estimated by using the associated α-particle method[3], which is the most accurate method to determine it.

In this method, the absolute neutron yield is estimated from the α-count detected by the α-detector, i.e., silicon surface barrier detector (SSD), and anisotropy correction factor is used to convert the α-count to the absolute neutron yield.

In the target used at the FNS, titanium layer in which the tritium is absorbed, is thick enough as compared with the range of incident deuteron. For thick target, anisotropy correction factor must be calculated from reaction kinematics considering the slowing down process of deuterons in titanium-tritium (Ti-T) layer.

In this report, calculations and error analyses are carried out for thick-target case considering following items :

(i) Energy loss data of deuteron in Ti-T target

(ii) Relativistic kinematics

(iii) Nonuniformity of tritium distribution in Ti-T target.

The relation between the neutron yield, α-count and the anisotropy correction factor is summarized in chapter 2. In chapter 3, calculational results of anisotropy correction factor are described and the accuracy of the anisotropy correction factor is discussed.

In appendix, the angular distribution of neutron are compiled in graphs and numerical tables.

2. Relation between Total Neutron Yield and α-count

The configuration of the α-detector and target assembly is shown in Fig. 1. The α-detector is placed at an angle θ_α to the incident deuteron, and subtending a solid angle $\Delta\Omega$ at the target. Parameters related to the SSD and the target are given in Table 1. The following discussions is extended for the 1st target room.

The total number of α particles produced in the target, Y_α, is given by

$$Y_\alpha = C_\alpha \cdot K, \tag{2.1}$$

where C_α is α counts detected by the SSD, and conversion factor K is defined by

$$K = \frac{4\pi}{\Delta\Omega} \cdot R_\alpha, \tag{2.2}$$

where R_α is the anisotropy correction factor whose value depends on the incident deuteron energy E_d and the angle θ_α.

The total neutron yield, Y_n, is equal to the total number of α-particles. The absolute total neutron yield Y_n is given by the relation :

$$Y_n = \frac{4\pi}{\Delta\Omega} \cdot C_\alpha \cdot R_\alpha(E_d, \theta_\alpha). \tag{2.3}$$

The uncertainties of $4\pi/\Delta\Omega$ and C_α are discussed separately in Ref. (3). In this work, calculations have been performed to examine the uncertainty of anisotropy correction factor.

The expression for the anisotropy correction factor is derived as follows [4] :

$$R_\alpha(E_d, \theta_\alpha) = \frac{\int_0^{E_d} (\frac{d\sigma}{d\omega'})(E) / (\frac{dE}{dx})_{Ti-T}(E)\,dE}{\int_0^{E_d} (\frac{d\sigma}{d\omega'})(E) / (\frac{dE}{dx})_{Ti-T}(E) (\frac{d\omega'}{d\omega})(E, \theta_\alpha)\,dE} , \qquad (2.4)$$

where $(d\sigma/d\omega')$ is the differential cross section of D-T reaction in the center-of-mass (CM) system [5] which is tabulated in Table 2,

$(dE/dx)_{Ti-T}$ the rate of energy loss of deuteron in a Ti-T target,

$(d\omega'/d\omega)$ the solid angle conversion factor for α-paticle from the CM system to the laboratory system (Lab system).

Following assumptions were taken in the derivation of this expression.

(i) The reaction products are emitted isotropically in the CM system,

(ii) Tritium atoms are loaded uniformly in the titanium layer,

(iii) Direction of reacting deuteron is taken to be that of the beam.

The errors due to the assumptions (i) and (iii) were evaluated to be less than 1%. [5]

In the present work, the error due to the assumption (ii) was estimated. Experimental data was adopted as the rate of energy loss of deuteron in Ti layer, which has been obtained by interpolation, and the effect on the anisotropy correction factor was examined. The calculations of the solid angle conversion factor were carried out basing upon nonrelativistic and relativistic kinematics, and the effect of relativistic kinematics on the anisotropy correction factor was examined.

The numerical integration in Eq.(2.4) was performed using $(d\sigma/d\omega')$, (dE/dx) and $(d\omega'/d\omega)$ data given at intervals of 5 keV.

3. Calculation of Anisotropy Correction Factor

3.1 Energy Loss Data of Deuteron in Ti-T Target

Assuming Bragg's law, i.e., the energy loss in a compound is the sum of the energy loss in its constituents, the rate of energy loss of deuteron in a Ti-T target is given by

$$\left(\frac{dE}{dx}\right)_{Ti-T} = \frac{48}{48+3N}\left(\frac{dE}{dx}\right)_{Ti} + \frac{3N}{48+3N}\left(\frac{dE}{dx}\right)_{T} , \qquad (3.1)$$

where $(dE/dx)_{Ti}$ is the rate of energy loss of deuterons in titanium, $(dE/dx)_{T}$ that in tritium, and N the number of tritium atoms per titanium atom.

In the earlier reports [4,5], the $(dE/dx)_{Ti}$ for proton was obtained by interpolating between proton data for Al and Cu with respect to $A^{-1/2}$ (A is atomic number), and the rate of energy loss is assumed to be only a function of the velocity of particles :

$$\left(\frac{dE}{dx}\right)_{proton}(E) = \left(\frac{dE}{dx}\right)_{deuteron}(2E) . \qquad (3.2)$$

The anisotropy correction factor has been calculated using the $(dE/dx)_{Ti}$ data for proton compiled by Ziegler [6], and also using Benveniste's data to compare the difference between both cases.

In both cases, the rate of energy loss of deuteron in tritium is derived from the rate of energy loss of proton in hydrogen.

The comparison between both cases is shown in Fig. 2 and Table 3. The cases 1 and 2 in Table 4 are the results using the data of Benveniste's old data, and Ziegler's new data, respectively. Though the difference of the value of $(dE/dX)_{Ti-T}$ is about 30 % in all energy range,

the calculation shows that there is only a 0.4 % change in $R_\alpha(E_d, \theta_\alpha=179.1°)$. The reason is that the (dE/dx) appears in both the numerator and denominator of Eq. (4).

The $(dE/dx)_{Ti-T}$ is a function of N. The calculated result shows that a change of N from 1.0 to 2.0 yields a 30 % change in $(dE/dx)_{Ti-T}$, while little change appears in R_α (See case 4-6 in Table 4). Thus we assumed N = 1.0 in the following calculations.

3.2 Relativistic Kinematics

The solid angle conversion factor from the CM system primed quantities to the Lab system is written as;

$$\frac{d\omega'}{d\omega} = \frac{\sin\theta' d\theta'}{\sin\theta\, d\theta} \tag{3.3}$$

Nonrelativistic Formulation

Basing upon nonrelativistic kinematics, the relation between the CM angle θ' and the Lab angle θ is

$$\cos\theta' = -\gamma\sin^2\theta + \cos\theta\sqrt{1-\gamma^2\sin^2\theta}\ , \tag{3.4}$$

where $\frac{1}{\gamma^2} = \frac{m_n}{m_\alpha}\frac{m_D+m_T}{m_D}\left(\frac{m_T}{m_D+m_T} + \frac{Q}{E_0}\right)$

m_D : mass of deuteron

m_T : mass of tritium atom

m_n : mass of neutron

m_α : mass of alpha particle

E_0 : incident energy of deuterons

Q : Q-value of reaction

Differentiating Eq. (3.4),

$$\sin\theta' d\theta' = \left(2\gamma\sin\theta\cos\theta + \sin\theta\sqrt{1-\gamma^2\sin^2\theta} + \frac{\gamma^2\sin\theta\cos^2\theta}{\sqrt{1-\gamma^2\sin^2\theta}}\right)d\theta\ . \tag{3.5}$$

Inserting Eq. (3.5) in Eq. (3.3)

$$\left(\frac{d\omega'}{d\omega}\right)_{NR} = \frac{\gamma\left(\cos\theta+\sqrt{1/\gamma^2 - \sin^2\theta}\right)^2}{\sqrt{1/\gamma^2 - \sin^2\theta}}\ . \tag{3.6}$$

Relativistic Formulation

Basing upon relativistic kinematics,

$$\tan\theta' = \frac{\sin\theta}{\gamma(\cos\theta - B)} \quad , \tag{3.7}$$

where $\gamma = 1/\sqrt{1-\beta^2}$, $B = \beta/\beta_3$, $\beta = P_1/(E_1+M_2)$, $\beta_3 = P_3/(T_3+M_3)$

P_1 : momentum of deuteron in Lab system

P_3 : momentum of alpha particle in Lab system

E_1 : kinetic energy of deuteron in Lab system

M_2 : mass of tritium atom

M_3 : mass of alpha particle.

Rearranging Eq.(3.7) ,

$$\cos\theta' = \frac{\gamma(\cos\theta - B)}{\sqrt{\gamma^2(\cos\theta - B)^2 + \sin^2\theta}} \quad . \tag{3.8}$$

Differentiating Eq.(3.8) ,

$$\sin\theta' d\theta' = \frac{\gamma(1 - B\cos\theta)\sin\theta d\theta}{\{\gamma^2(\cos\theta - B)^2 + \sin^2\theta\}^{3/2}} \tag{3.9}$$

Inserting Eq. (3.9) in Eq. (3.3),

$$\left(\frac{d\omega'}{d\omega}\right)_{R.} = \frac{\gamma(1 - B\cos\theta)}{\{\gamma^2(\cos - B)^2 + \sin^2\theta\}^{3/2}} \quad . \tag{3.10}$$

The values of $\left(\frac{d\omega'}{d\omega}\right)_{NR}$ and $\left(\frac{d\omega'}{d\omega}\right)_{R}$ are shown in Table 5. The anisotropy correction factors $R_\alpha(E_d, \theta_\alpha = 179.1°)$ calculated using $\left(\frac{d\omega'}{d\omega}\right)_{NR}$ and $\left(\frac{d\omega'}{d\omega}\right)_{R}$ are shown in case 2 and case 4 of Table 4 respectively. It is revealed from Table 4 that the effect of relativistic kinematics on anisotropy correction factor is less than 0.2 %.

3.3 Effect of Nonuniformity in the Tritium Distribution

The tritium distribution with depth in the target was assumed to be constant in the above calculations. It is not uniform actually by releasing the tritium atoms from the surface and replacing them by the deuterons due to the bombarding beam. Considering the nonuniformity of tritium distribution in the target, the expression for R_α becomes

$$R_\alpha(E_d, \theta_\alpha) = \frac{\int_0^{E_d} (\frac{d\alpha}{d\omega'})(E)/(\frac{dE}{dx})_{Ti-T}(E) n_T(E(x))dE}{\int_0^{E_d} (\frac{d\sigma}{d\omega'})(E)/(\frac{dE}{dx})_{Ti-T}(E)(\frac{d\omega'}{d\omega})(E,\theta_\alpha) n_T(E(x))dE}, \quad (3.11)$$

where $n_T(E(x))$ represents the tritium distribution.

The effect of tritium distribution was examined by calculating the anisotropy correction factor for simplified models as follows.

Model (A)

The lack of tritium atoms in the surface layer is assumed to be the distribution in Fig. 3(a) as the function of distance x from surface. As the deuteron energy E decreases with the penetrating length x, the distribution can be written in Fig. 3(b) as the function of E. The function of $n_T(x(E))$ and $n_T(E(x))$ can be expressed as the following forms :

$$n_T(x(E)) = \begin{cases} 0 & 0 < x < \Delta x \\ 1 & \Delta x < x \end{cases} \quad (3.12)$$

or

$$n_T(E(x)) = \begin{cases} 1 & 0 < E < E_d - \Delta E_d \\ 0 & E_d - \Delta E_d < E < E_d \end{cases} \quad (3.13)$$

It is clear that the existence of surface layer lacking of tritium affects on the integrals in Eq. (3.11) by lowering the value of the upper

limit E_d and the value of R_α is reduced. The calculated results of R_α for several value of E_d and ΔE_d are summarized in Table 6. In case that E_d = 400 keV, the value of R_α reduces about 2.8 % for Δx = 0.48 mg/cm^2. This value of Δx is determined by taking account of the experiment.[7]

Model (B)

The tritium depletion with depth in the target is considered in this case. The tritium distribution used in this model is shown in Fig. 3(c) or (d). This curve is based on the experiments.[7] The function of $n_T(x(E))$ and $n_T(E(x))$ are given by

$$n_T(x(E)) = \begin{cases} \dfrac{a}{x_a}x & 0 < x < x_a \\ -\dfrac{a-b}{x_b-x_a}x + \dfrac{ax_b-bx_a}{x_b-x_a} & x_a < x < x_b \\ \dfrac{1-b}{x_c-x_b}x + \dfrac{bx_c-x_b}{x_c-x_b} & x_b < x < x_c \\ 1.0 & x_c < x \end{cases}, \tag{3.14}$$

or

$$n_T(E(x)) = \begin{cases} \dfrac{a-b}{E_a}E + b & 0 < E < E_a \\ -\dfrac{a}{E_d-E_a}E + \dfrac{aE_d}{E_d-E_a} & E_a < E < E_d \end{cases}, \tag{3.15}$$

where the parameters a and b determine the profile of tritium distribution.

An experimental result of tritium depth profile shows that the depletion of tritium is most severe near the end of 1.6 mg/cm^2 range of 400 keV deuterons, and the value of x_a is about 1.0 mg/cm^2.[7]

The deuteron energy at the position of x_a is estimated as follows. In the distance between x and x+Δx, the deuteron losses its energy ΔE (mainly by Ti) and the relation is approximately given by

$$\Delta X = \left(\frac{\Delta X}{\Delta E}\right)_{Ti} \Delta E = \left(\frac{dE}{dX}\right)^{-1} \Delta E \quad . \tag{3.16}$$

In accordance with the assumption (iii) described in section 2, the deuterons go straight and its track length equal to the projected range. The distance x from the surface to the point where the deuteron slow down to the energy E is given by

$$X = \sum_{E_d} \Delta X \quad . \tag{3.17}$$

The relation between E and x is shown in Table 7 and Fig. 4 using Ziegler's data as $(dE/dx)_{Ti}$.

From Fig. 4, the deuteron energy is 35 keV at the position x_a=1.0 mg/cm^2. The anisotropy correction factor R_α in the case that E_d=400 keV and E_a=35 keV is calculated for several values of a and b, and summarized in Table 8. To examine the effect of uncertainty in the (dE/dx), the calculation for E_a=100 keV is carried out. The calculated results show that R_α does not change very much with the parameters a and b but with the parameter E_a. In Table 9 and Fig. 5, $R_\alpha(E_d, E_a, \theta_\alpha=179.1°)$ is shown as a function of E_a (a=0.8,b=0.6) in the case of E_d = 300,350,400 keV. In case that E_d=400 keV, the difference of R_α is about 3 % between an ideal model (a=b=1, $E_a=E_d$=400 keV) and a used target model (a=0.6, b=0.4,E_a= 35 keV). Although actual tritium profile in a target can not be measured on-line and varies from the initial state to the final state, we must assume the profile to determine the factor R_α. So we have selected the parameters 0.8, 0.6 and 1/2 E_d for a, b and E_a, respectively. The actual value of conversion factor R_α must be between those of ideal and ending profiles. Therefore the error of R_α using the Model (B) is within about

$\pm$ 1.5 % (= 3/2 %).

The factor R_α and its maximum error are shown in Table 10. Here, we have adopted the Model (B) as the model of nonuniform tritium distribution, because, (1) the Model (B) resembles actual profile more than Model (A), (2) the error in case of Model (B) is greater than that of Model (A), so the error is estimated more over than the Model (A).

4. Summary

The calculations of anisotropy correction factor and the estimation of its error are carried out to determine the absolute neutron yield by the associated α-particle method for thick-target case.

The examined items are as follows :

(i) Energy loss data of deuteron in Ti-T target

(ii) Relativistic kinematics

(iii) Nonuniformity of tritium distribution in Ti-T target.

The calculations show that the error is less than 0.4 %, 0.2 % and ± 1.5 % for (i), (ii) and (iii) respectively.

Through these calculations, it is concluded that, the anisotropy correction factor has the uncertainty of about ± 1.5 % mainly due to the nonuniformity of the tritium distribution caused by depletion of tritium atoms developed by bombardment of deuteron beam in Ti-T layer.

In appendix, the angular distribution of neutron, average reaction energy are compiled in numerical tables.

Acknowledgment

The authors thank Drs. T.Nakamura and Y.Ikeda for the valuable discussion on this work.

4. Summary

The calculations of anisotropy correction factor and the estimation of its error are carried out to determine the absolute neutron yield by the associated α-particle method for thick-target case.

The examined items are as follows :

(i) Energy loss data of deuteron in Ti-T target

(ii) Relativistic kinematics

(iii) Nonuniformity of tritium distribution in Ti-T target.

The calculations show that the error is less than 0.4 %, 0.2 % and ± 1.5 % for (i), (ii) and (iii) respectively.

Through these calculations, it is concluded that, the anisotropy correction factor has the uncertainty of about ± 1.5 % mainly due to the nonuniformity of the tritium distribution caused by depletion of tritium atoms developed by bombardment of deuteron beam in Ti-T layer.

In appendix, the angular distribution of neutron, average reaction energy are compiled in numerical tables.

Acknowledgment

The authors thank Drs. T.Nakamura and Y.Ikeda for the valuable discussion on this work.

References

(1) Nakamura, T., et al. : "Futions Neusronics Source (FNS)", Proc. 3rd Symp. on Accelerator Sci. & Technol., Osaka Univ., Aug. 27-29, 1980, pp. 55-56.

(2) Nakamura, T., et al. : "Present Status of the Fusion Neutronics Source (FNS)", Proc. 4th Sym. on Accelerator Sci. & Technol., RIKEN, Saitama, Nov. 24-26, 1982, pp. 155-156

(3) Maekawa, H., et al. : JAERI-M 83-219, (1983)

(4) Benveniste J., Zengen J. : UCRL-4266 (1954)

(5) Benveniste J., Mitchell A.C., Schrader C.D., Zenger J.H. : Nucl. Instr. Meth. 7 (1960) 306.

(6) Andersen H.H., Ziegler J.F. : "The Stopping Power and Ranges of Ion in Matter Vol.3" ed. Ziegler J.F., Pergamon, New York (1977)

(7) Davis J.C., Anderson J.D.: J. Vac. Sci. Technol. 12 (1975) 358.

Table 1 Parameters related to arrangement of Ti-T target and α detector for the 1st and the 2nd target rooms.

	1st target room	2nd target room
a [mm]	1.0246 ± 0.0026 *	1.395 ± 0.004
L [mm]	1578 ± 1	956.2 ± 2
r [mm]	25 ± 1	27.2 ± 1
$\theta_\alpha (=\tan^{-1}(r/L))$ [deg]	179.1 ± 0.03	178.4 ± 0.06
$\Delta\Omega = \frac{\pi(a/2)^2\cos\theta}{L^2 + r^2}$ [sr]	$(3.310 \pm 0.034) \times 10^{-7}$ *	$(1.670 \pm 0.010) \times 10^{-6}$

* Before April 1984, values of a and $\Delta\Omega$ for the 1st target room were $a=0.9835 \pm 0.0054$, $\Delta\Omega=(3.050 \pm 0.034) \times 10^{-7}$ respectively.

Table 2 Differential cross section values for $^{3}T(d,n)^{4}He$ reaction

E_d [keV]	$(\frac{d\sigma}{d\omega},)$ [mb/sr]	E_d [keV]	$(\frac{d\sigma}{d\omega},)$ [mb/sr]
5	0.0	255	128.0
10	0.1	260	122.0
15	0.2	265	118.0
20	4.3	270	114.0
25	12.0	275	110.0
30	19.6	280	106.0
35	34.0	285	103.0
40	52.9	290	100.0
45	70.0	295	97.6
50	106.0	300	95.2
55	141.0	305	93.2
60	175.0	310	91.1
65	213.0	315	89.2
70	250.0	320	87.3
75	283.0	325	85.6
80	315.0	330	83.8
85	341.0	335	82.2
90	367.0	340	80.6
95	381.0	345	79.1
100	394.0	350	77.5
105	397.0	355	75.9
110	399.0	360	74.3
115	393.0	365	72.8
120	387.0	370	71.3
125	377.0	375	70.0
130	367.0	380	68.6
135	353.0	385	67.3
140	339.0	390	65.9
145	328.0	395	64.7
150	317.0	400	63.5
155	302.0	405	62.3
160	286.0	410	61.1
165	274.0	415	60.0
170	262.0	420	58.9
175	249.0	425	57.9
180	236.0	430	56.8
185	226.0	435	55.9
190	215.0	440	54.9
195	207.0	445	54.0
200	199.0	450	53.0
205	190.0	455	52.2
210	181.0	460	51.3
215	174.0	465	50.6
220	167.0	470	49.8
225	160.0	475	49.1
230	153.0	480	48.3
235	148.0	485	47.6
240	142.0	490	46.9
245	138.0	495	46.2
250	133.0	500	45.5

Table 3 The rate of energy loss of deuterons in Ti, T and Ti-T

E_d[keV]	$(\frac{dE}{dx})_{Ti}$	$(\frac{dE}{dx})_{T}$	$(\frac{dE}{dx})_{Ti-T}$	$(\frac{dE}{dx})^{old}_{Ti-T}$
10	1.420E+02	5.959E+02	1.687E+02	9.500E+01
20	1.929E+02	8.014E+02	2.287E+02	1.600E+02
30	2.299E+02	9.420E+02	2.718E+02	2.000E+02
40	2.592E+02	1.046E+03	3.055E+02	2.220E+02
50	2.835E+02	1.124E+03	3.329E+02	2.450E+02
60	3.039E+02	1.182E+03	3.554E+02	2.600E+02
70	3.209E+02	1.225E+03	3.741E+02	2.760E+02
80	3.354E+02	1.255E+03	3.895E+02	2.880E+02
90	3.475E+02	1.275E+03	4.021E+02	3.000E+02
100	3.577E+02	1.287E+03	4.123E+02	3.100E+02
110	3.660E+02	1.291E+03	4.204E+02	3.180E+02
120	3.728E+02	1.290E+03	4.267E+02	3.250E+02
130	3.781E+02	1.285E+03	4.314E+02	3.280E+02
140	3.821E+02	1.275E+03	4.347E+02	3.320E+02
150	3.851E+02	1.262E+03	4.367E+02	3.340E+02
160	3.870E+02	1.247E+03	4.376E+02	3.340E+02
170	3.880E+02	1.231E+03	4.376E+02	3.350E+02
180	3.883E+02	1.212E+03	4.368E+02	3.350E+02
190	3.879E+02	1.193E+03	4.353E+02	3.340E+02
200	3.869E+02	1.173E+03	4.331E+02	3.330E+02
210	3.854E+02	1.152E+03	4.305E+02	3.320E+02
220	3.834E+02	1.132E+03	4.274E+02	3.310E+02
230	3.811E+02	1.111E+03	4.240E+02	3.290E+02
240	3.785E+02	1.090E+03	4.203E+02	3.280E+02
250	3.756E+02	1.069E+03	4.164E+02	3.260E+02
260	3.725E+02	1.048E+03	4.122E+02	3.240E+02
270	3.692E+02	1.028E+03	4.079E+02	3.220E+02
280	3.658E+02	1.008E+03	4.036E+02	3.190E+02
290	3.622E+02	9.886E+02	3.991E+02	3.170E+02
300	3.586E+02	9.695E+02	3.946E+02	3.150E+02
310	3.550E+02	9.509E+02	3.900E+02	3.130E+02
320	3.513E+02	9.327E+02	3.855E+02	3.110E+02
330	3.476E+02	9.150E+02	3.810E+02	3.090E+02
340	3.439E+02	8.978E+02	3.765E+02	3.070E+02
350	3.402E+02	8.811E+02	3.720E+02	3.050E+02
360	3.365E+02	8.649E+02	3.676E+02	3.020E+02
370	3.329E+02	8.491E+02	3.633E+02	3.000E+02
380	3.293E+02	8.338E+02	3.590E+02	2.980E+02
390	3.258E+02	8.190E+02	3.548E+02	2.960E+02
400	3.223E+02	8.046E+02	3.507E+02	2.940E+02
410	3.189E+02	7.906E+02	3.466E+02	2.920E+02
420	3.155E+02	7.771E+02	3.426E+02	2.900E+02
430	3.122E+02	7.640E+02	3.388E+02	2.880E+02
440	3.089E+02	7.513E+02	3.350E+02	2.860E+02
450	3.058E+02	7.390E+02	3.312E+02	2.840E+02
460	3.027E+02	7.270E+02	3.276E+02	2.820E+02
470	2.996E+02	7.155E+02	3.241E+02	2.800E+02
480	2.966E+02	7.042E+02	3.206E+02	2.780E+02
490	2.937E+02	6.934E+02	3.172E+02	2.760E+02
500	2.909E+02	6.828E+02	3.139E+02	2.740E+02

Table 4 Anisotropy Correction Factor $R_\alpha(E_d, \theta_\alpha = 179.1°)$

E_d [keV]		case 1	case 2	case 3	case 4	case 5	case 6
	(dE/dx)	old	new	old	new	new	new
	(dω'/dω)	NR	NR	R	R	R	R
	N	1.0	1.0	1.0	1.0	1.5	2.0
10		1.0631	1.0631	1.0635	1.0635	1.0635	1.0635
20		1.0884	1.0888	1.0889	1.0894	1.0894	1.0894
30		1.1044	1.1049	1.1050	1.1055	1.1055	1.1055
40		1.1196	1.1198	1.1203	1.1205	1.1205	1.1205
50		1.1332	1.1334	1.1340	1.1342	1.1342	1.1343
60		1.1458	1.1459	1.1467	1.1468	1.1468	1.1469
70		1.1573	1.1574	1.1582	1.1583	1.1584	1.1585
80		1.1677	1.1679	1.1688	1.1689	1.1690	1.1690
90		1.1772	1.1774	1.1783	1.1785	1.1786	1.1787
100		1.1859	1.1861	1.1870	1.1873	1.1874	1.1875
110		1.1937	1.1940	1.1948	1.1952	1.1953	1.1955
120		1.2007	1.2011	1.2019	1.2023	1.2025	1.2027
130		1.2070	1.2075	1.2083	1.2088	1.2090	1.2093
140		1.2128	1.2134	1.2141	1.2147	1.2150	1.2152
150		1.2181	1.2187	1.2195	1.2201	1.2204	1.2207
160		1.2230	1.2237	1.2244	1.2251	1.2255	1.2258
170		1.2278	1.2284	1.2292	1.2299	1.2303	1.2307
180		1.2321	1.2328	1.2335	1.2343	1.2347	1.2352
190		1.2359	1.2367	1.2374	1.2382	1.2387	1.2392
200		1.2396	1.2403	1.2411	1.2419	1.2424	1.2430
210		1.2430	1.2438	1.2445	1.2454	1.2460	1.2466
220		1.2462	1.2471	1.2478	1.2487	1.2494	1.2500
230		1.2493	1.2502	1.2509	1.2518	1.2526	1.2532
240		1.2522	1.2532	1.2538	1.2548	1.2556	1.2564
250		1.2550	1.2561	1.2567	1.2577	1.2586	1.2594
260		1.2577	1.2589	1.2594	1.2605	1.2614	1.2623
270		1.2603	1.2615	1.2619	1.2632	1.2641	1.2650
280		1.2628	1.2641	1.2644	1.2658	1.2668	1.2677
290		1.2652	1.2666	1.2668	1.2682	1.2693	1.2703
300		1.2675	1.2690	1.2692	1.2707	1.2718	1.2729
310		1.2698	1.2714	1.2715	1.2731	1.2743	1.2754
320		1.2720	1.2737	1.2738	1.2755	1.2767	1.2779
330		1.2743	1.2761	1.2760	1.2778	1.2791	1.2804
340		1.2764	1.2784	1.2782	1.2802	1.2815	1.2828
350		1.2786	1.2807	1.2804	1.2825	1.2839	1.2852
360		1.2807	1.2829	1.2825	1.2847	1.2862	1.2876
370		1.2828	1.2852	1.2846	1.2870	1.2885	1.2900
380		1.2849	1.2874	1.2867	1.2892	1.2908	1.2923
390		1.2869	1.2895	1.2887	1.2914	1.2931	1.2946
400		1.2889	1.2917	1.2907	1.2936	1.2953	1.2969
410		1.2908	1.2938	1.2927	1.2957	1.2975	1.2992
420		1.2928	1.2959	1.2946	1.2978	1.2997	1.3014
430		1.2947	1.2980	1.2966	1.2999	1.3018	1.3036
440		1.2965	1.3000	1.2984	1.3020	1.3040	1.3058
450		1.2984	1.3020	1.3003	1.3040	1.3061	1.3080
460		1.3003	1.3041	1.3021	1.3060	1.3081	1.3101
470		1.3020	1.3060	1.3039	1.3080	1.3102	1.3123
480		1.3038	1.3080	1.3057	1.3100	1.3122	1.3144
490		1.3056	1.3100	1.3075	1.3120	1.3143	1.3166
500		1.3072	1.3119	1.3092	1.3139	1.3163	1.3185

Table 5 Solid angle conversion factor calculated by the use of nonrelativistic (NR) and relativistic (R) kinematics

E_d [keV]	$(\frac{d\omega}{d\omega'})_{NR}$	$(\frac{d\omega}{d\omega'})_{R}$
10	0.9406241	0.9403061
20	0.9163752	0.9161329
30	0.8933434	0.8928075
40	0.8831229	0.8825102
50	0.8693277	0.8691489
60	0.8579011	0.8571637
70	0.8470113	0.8462207
80	0.8369431	0.8361042
90	0.8275465	0.8266625
100	0.8187124	0.8177866
110	0.8103530	0.8093932
120	0.8024195	0.8014177
130	0.7948462	0.7938095
140	0.7875966	0.7865264
150	0.7806365	0.7795348
160	0.7739377	0.7728059
170	0.7674759	0.7663149
180	0.7612305	0.7600417
190	0.7551833	0.7539689
200	0.7493206	0.7480798
210	0.7436271	0.7423615
220	0.7380913	0.7368018
230	0.7327026	0.7313902
240	0.7274518	0.7261170
250	0.7223301	0.7209737
260	0.7173299	0.7159525
270	0.7124443	0.7110466
280	0.7076670	0.7062494
290	0.7029924	0.7015557
300	0.6984150	0.6969595
310	0.6939303	0.6924565
320	0.6895335	0.6880420
330	0.6852208	0.6837122
340	0.6809883	0.6794629
350	0.6768324	0.6752908
360	0.6727502	0.6711922
370	0.6687384	0.6671649
380	0.6647941	0.6632054
390	0.6609147	0.6593112
400	0.6570979	0.6554795
410	0.6533412	0.6517089
420	0.6496425	0.6479961
430	0.6459997	0.6443397
440	0.6424110	0.6407375
450	0.6388743	0.6371873
460	0.6353881	0.6336887
470	0.6319507	0.6302390
480	0.6285606	0.6268365
490	0.6252162	0.6234801
500	0.6219163	0.6201682

Table 6 Anisotropy correction factor $R_\alpha(E_d$=400 keV, θ_α=179.1°) considering nonuniformity of tritium distribution in target [Model(A)]

ΔE_d [keV]	0	50	100	150
ΔX [mg/cm^2]	0	0.16	0.32	0.48
E_d = 200 [keV]	1.242	1.220(-1.7%)	1.187(-4.4%)	1.134(-8.7%)
250	1.258	1.242(-1.3%)	1.220(-3.0%)	1.187(-5.6%)
300	1.271	1.258(-1.0%)	1.242(-2.3%)	1.220(-4.0%)
350	1.282	1.271(-0.9%)	1.258(-2.0%)	1.242(-3.2%)
400	1.294	1.282(-0.9%)	1.271(-1.8%)	1.252(-2.8%)

Table 7 Relation between deuteron energy and depth in Ti layer for the incident energy of 400 keV

E_d[keV]	$(\frac{dE}{dx})_{Ti}$[keV/mg/cm^2]	ΔX [mg/cm^2]	X [mg/cm^2]
400	3.2229E+02	3.1028E-02	3.1028E-02
390	3.2578E+02	3.0696E-02	6.1723E-02
380	3.2932E+02	3.0366E-02	9.2089E-02
370	3.3291E+02	3.0038E-02	1.2213E-01
360	3.3654E+02	2.9714E-02	1.5184E-01
350	3.4020E+02	2.9394E-02	1.8124E-01
340	3.4389E+02	2.9079E-02	2.1032E-01
330	3.4759E+02	2.8769E-02	2.3908E-01
320	3.5130E+02	2.8466E-02	2.6755E-01
310	3.5499E+02	2.8170E-02	2.9572E-01
300	3.5864E+02	2.7883E-02	3.2360E-01
290	3.6224E+02	2.7606E-02	3.5121E-01
280	3.6577E+02	2.7340E-02	3.7855E-01
270	3.6919E+02	2.7086E-02	4.0564E-01
260	3.7247E+02	2.6845E-02	4.3248E-01
250	3.7553E+02	2.6625E-02	4.5911E-01
240	3.7848E+02	2.6422E-02	4.8553E-01
230	3.8111E+02	2.6239E-02	5.1177E-01
220	3.8343E+02	2.6080E-02	5.3785E-01
210	3.8538E+02	2.5948E-02	5.6380E-01
200	3.8689E+02	2.5847E-02	5.8964E-01
190	3.8790E+02	2.5780E-02	6.1542E-01
180	3.8831E+02	2.5753E-02	6.4118E-01
170	3.8804E+02	2.5771E-02	6.6695E-01
160	3.8699E+02	2.5840E-02	6.9279E-01
150	3.8506E+02	2.5970E-02	7.1876E-01
140	3.8214E+02	2.6169E-02	7.4493E-01
130	3.7808E+02	2.6449E-02	7.7138E-01
120	3.7276E+02	2.6827E-02	7.9820E-01
110	3.6601E+02	2.7322E-02	8.2553E-01
100	3.5767E+02	2.7959E-02	8.5348E-01
90	3.4753E+02	2.8773E-02	8.8226E-01
80	3.3537E+02	2.9818E-02	9.1208E-01
70	3.2090E+02	3.1163E-02	9.4324E-01
60	3.0376E+02	3.2921E-02	9.7616E-01
50	2.8345E+02	3.5279E-02	1.0114E+00
40	2.5924E+02	3.8574E-02	1.0500E+00
30	2.2988E+02	4.3500E-02	1.0935E+00
20	1.9294E+02	5.1830E-02	1.1453E+00
10	1.4196E+02	7.0445E-02	1.2158E+00

Table 8 Anisotropy correction factor $R_\alpha(E_d$=400 keV, θ_α=179.1°) considering nonuniformity of tritium distribution in target [Model (B)]

E_a [keV]	b \ a	1.0	0.8	0.6	0.4
400	1.0	1.294			
100	0.8	1.262(-2.5%)	1.260(-2.6%)		
	0.6	1.263(-2.4%)	1.262(-2.5%)	1.260(-2.6%)	
	0.4	1.265(-2.2%)	1.264(-2.3%)	1.263(-2.4%)	1.260(-2.6%)
	0.2	1.267(-2.1%)	1.267(-2.1%)	1.266(-2.2%)	1.264(-2.3%)
35	0.8	1.258(-2.8%)	1.258(-2.8%)		
	0.6	1.258(-2.8%)	1.258(-2.8%)	1.258(-2.8%)	
	0.4	1.258(-2.8%)	1.258(-2.8%)	1.258(-2.8%)	1.258(-2.8%)
	0.2	1.258(-2.8%)	1.258(-2.8%)	1.258(-2.8%)	1.258(-2.8%)

Table 9 Anisotropy correction factor $R_\alpha(E_d, \theta_\alpha$ =179.1°, E_a, a=0.8, b=0.6) for the Model (B)

E_d [keV]	E_a [keV]	R_α
300	10	1.2403
	30	1.2403
	50	1.2408
	75	1.2425
	100	1.2458
	125	1.2498
	150	1.2539
	175	1.2581
	200	1.2618
	225	1.2656
	250	1.2689
	275	1.2724
350	10	1.2494
	30	1.2494
	50	1.2499
	75	1.2514
	100	1.2544
	125	1.2580
	150	1.2618
	175	1.2656
	200	1.2692
	225	1.2727
	250	1.2759
	275	1.2790
	300	1.2820
	325	1.2852
400	10	1.2575
	30	1.2575
	50	1.2579
	75	1.2594
	100	1.2621
	125	1.2655
	150	1.2691
	175	1.2727
	200	1.2762
	225	1.2795
	250	1.2826
	275	1.2856
	300	1.2885
	325	1.2915
	350	1.2943
	375	1.2974
	390	1.2988

Table 10 Anisotropy correction factor $R_\alpha(E_d, \Theta_\alpha = 179.1°, E_a = 1/2E_d, a=0.8, b=0.6)$ for the Model (B)

E_d [keV]	R_0 *1	R_α	Error [%] *2
200	1.2417	1.2239	1.45
205	1.2435	1.2257	1.45
210	1.2452	1.2275	1.44
215	1.2469	1.2292	1.44
220	1.2485	1.2310	1.42
225	1.2501	1.2326	1.42
230	1.2517	1.2343	1.41
235	1.2532	1.2359	1.40
240	1.2547	1.2374	1.40
245	1.2562	1.2389	1.40
250	1.2577	1.2405	1.39
255	1.2591	1.2419	1.38
260	1.2605	1.2433	1.38
265	1.2618	1.2448	1.37
270	1.2632	1.2462	1.36
275	1.2645	1.2475	1.36
280	1.2657	1.2488	1.35
285	1.2670	1.2501	1.35
290	1.2683	1.2515	1.34
295	1.2695	1.2528	1.33
300	1.2707	1.2539	1.34
305	1.2719	1.2552	1.33
310	1.2731	1.2564	1.33
315	1.2743	1.2577	1.32
320	1.2755	1.2588	1.33
325	1.2767	1.2600	1.33
330	1.2779	1.2611	1.33
335	1.2791	1.2623	1.33
340	1.2802	1.2634	1.33
345	1.2814	1.2645	1.34
350	1.2825	1.2656	1.34
355	1.2837	1.2667	1.34
360	1.2848	1.2678	1.34
365	1.2860	1.2689	1.35
370	1.2871	1.2700	1.35
375	1.2882	1.2710	1.35
380	1.2893	1.2720	1.36
385	1.2904	1.2731	1.36
390	1.2915	1.2741	1.37
395	1.2926	1.2752	1.36
400	1.2937	1.2761	1.38

*1 The factor for the ideal tritium profile

*2 This error means difference between R_o and R_α. The error of R_α can be less than this value.

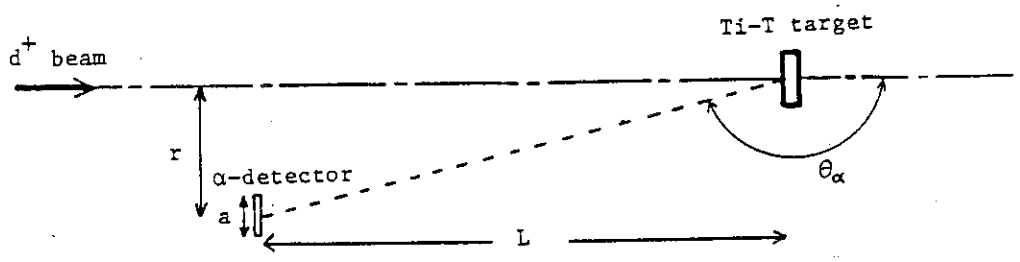

Fig. 1 Arrangement of Ti-T target and α-detector

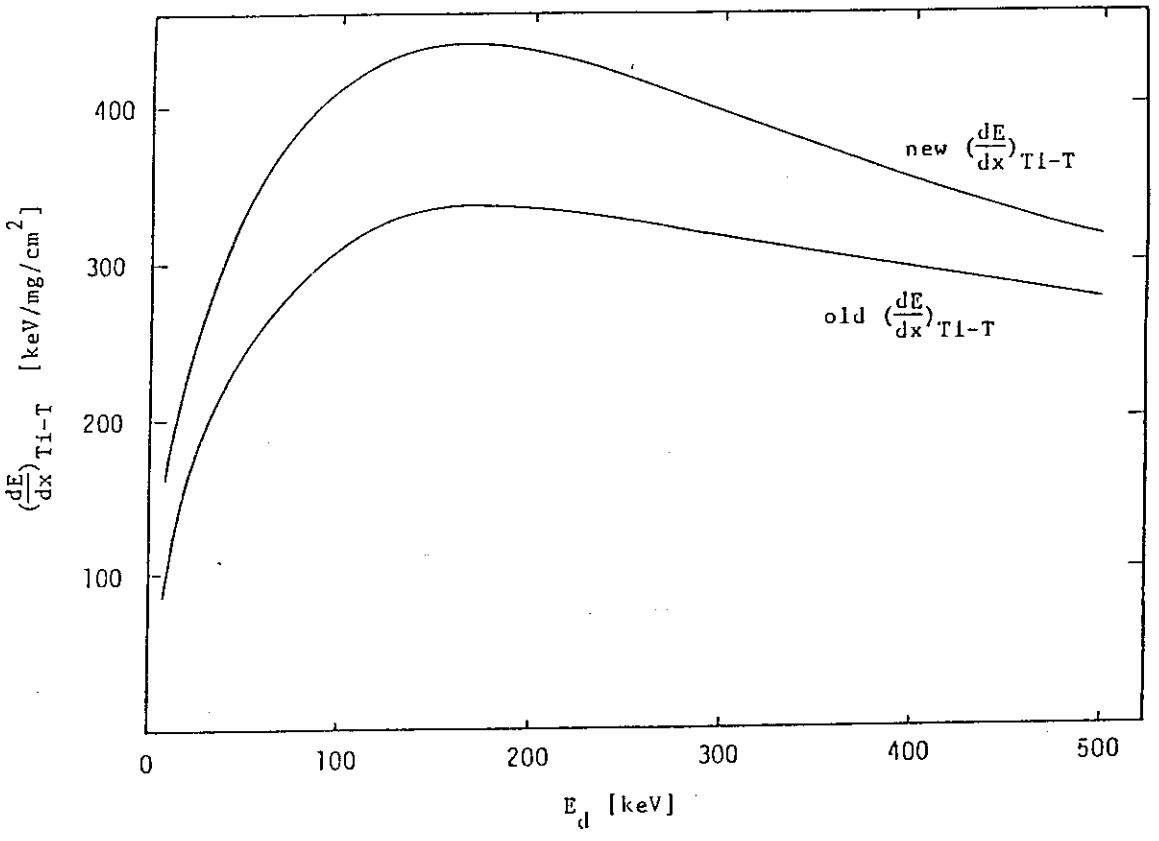

Fig. 2 The rate of energy loss of deuterons in Ti-T target

Model (A)

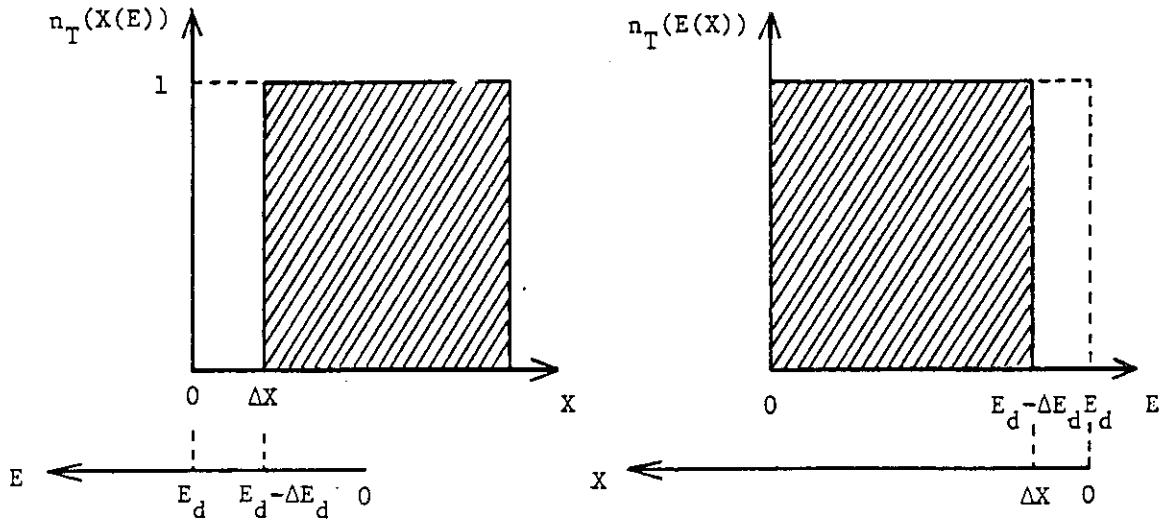

Model (B)

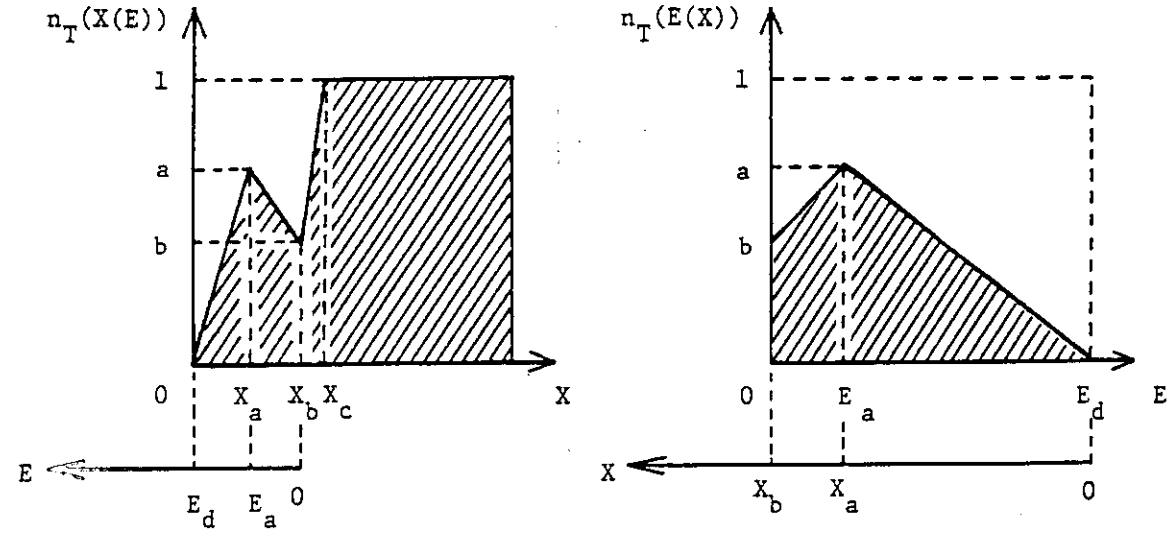

Fig. 3 Models of tritium depth profile

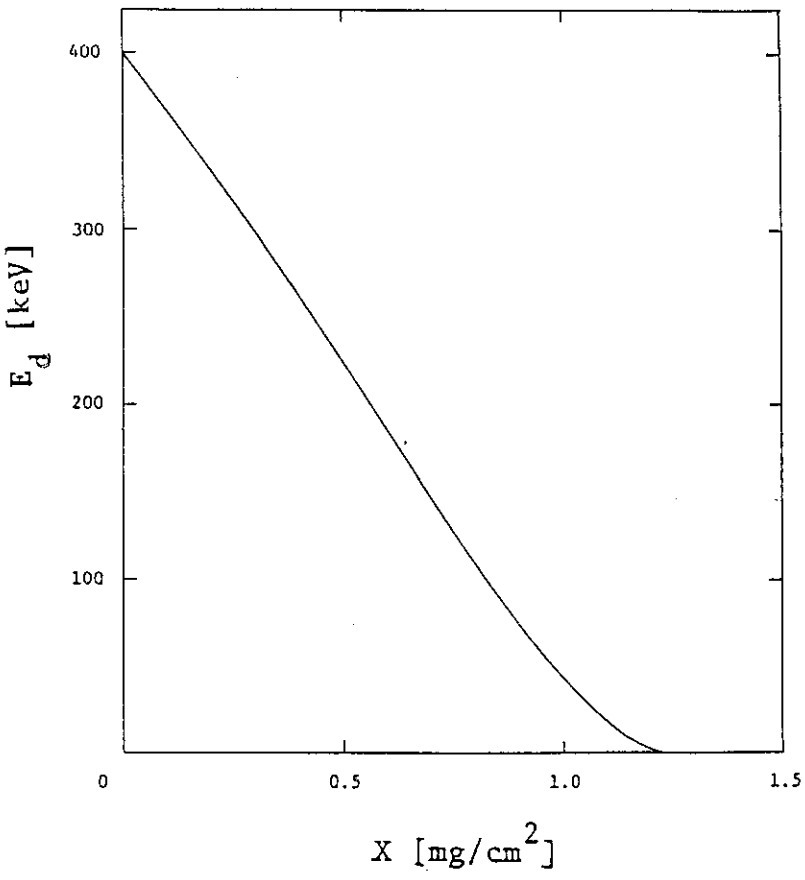

Fig 4 Relation between deuteron energy and depth in Ti layer for the incident energy of 400 keV

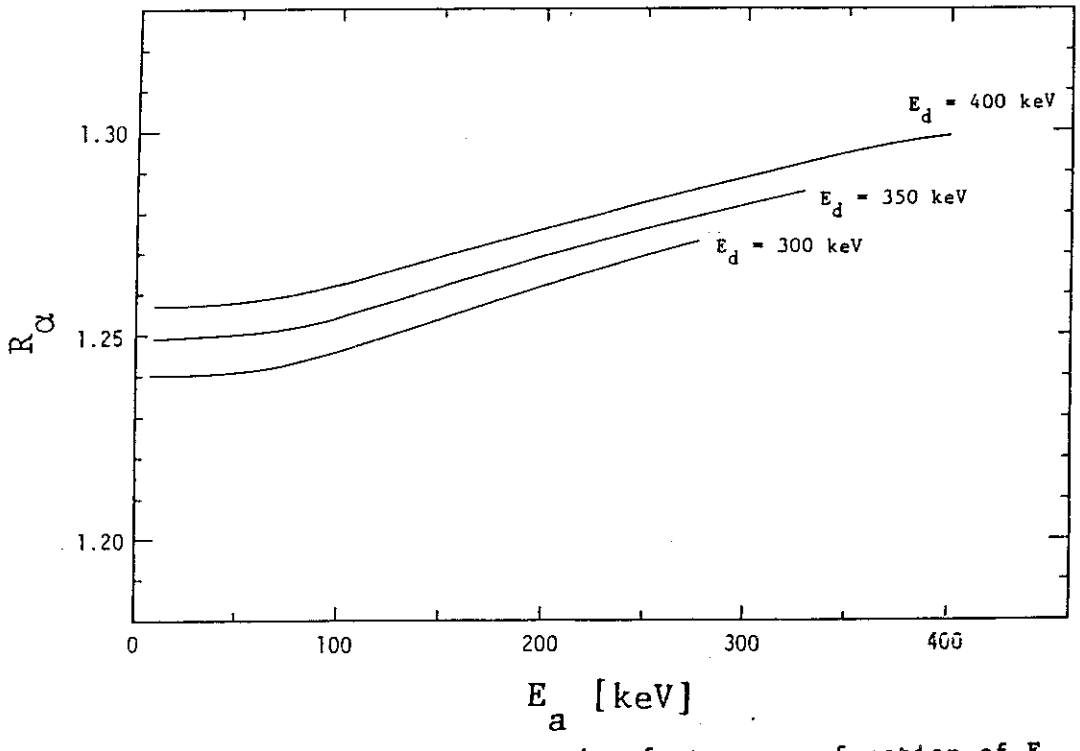

Fig. 5 Anisotropy correction factor as a function of E_a

Appendix 1 The Total Neutron Yield per Detected α-particle

The total neutron yield per detected α-particle, K, in FNS is

$$K = \frac{4\pi}{\Delta\Omega} \cdot R_\alpha(E_d, \theta_\alpha)$$

$$= \begin{cases} \dfrac{4\pi}{3.310\times10^{-7}} \cdot R_\alpha & \text{for the 1st Target room} \\ \dfrac{4\pi}{1.670\times10^{-6}} \cdot R_\alpha & \text{for the 2nd Target Room} \end{cases} \qquad (A.1.1)$$

The values of K are tabulated in Table A.1. Anisotropy correction factor R_α was calculated for the Model (B) (a=0.8, b=0.6 and E_a=1/2E_d).

Then, the total neutron yield Y_n can be obtained by multiplying α-count C_α by K :

$$Y_n = C_\alpha \cdot K. \qquad (A.1.2)$$

Appendix 2 Angular Distribution of Neutron

Relative intensity of neutron emitted in the direction of angle θ_n normalized to the intensity for $\theta_n = 0°$, $I(\theta_n)/I(0°)$, is given by the following equation :

$$\frac{I(\theta_n)}{I(0°)} = \frac{\int_0^{E_d} \left(\frac{d\sigma}{d\omega}\right) / \left(\frac{dE}{dx}\right) \cdot \left(\frac{d\omega'}{d\omega}\right)_n (E, \theta_n) dE}{\int_0^{E_d} \left(\frac{d\sigma}{d\omega}\right) / \left(\frac{dE}{dx}\right) \cdot \left(\frac{d\omega'}{d\omega}\right)_n (E, 0°) dE}$$

$$\approx \frac{\int_0^{E_d} \left(\frac{d\sigma}{d\omega}\right) / \left(\frac{dE}{dx}\right) \cdot \left(\frac{d\omega'}{d\omega}\right)_n (E, \theta_n) dE}{\int_0^{E_d} \left(\frac{d\sigma}{d\omega}\right) / \left(\frac{dE}{dx}\right) dE} = \left\langle \left(\frac{d\omega'}{d\omega}\right)_n \right\rangle ,$$

$$\frac{I(\theta_n)}{I(0°)} \approx \left\langle \left(\frac{d\omega'}{d\omega}\right)_n \right\rangle , \qquad \text{(A.2.1)}$$

where $(d\omega'/d\omega)_n(E, \theta_n)$ is the solid angle conversion factor for D-T neutron which is obtained by exchanging M_2 and M_3 in Eq. (3.7). Other notations are the same as Eq. (2.4).

The values of $\langle (d\omega'/d\omega)_n \rangle$ are tabulated in Table A.2 for uniform distribution and for the Model (B) (a=0.8, b=0.6 and $E_a = 1/2\ E_d$) as the tritium distribution in case that E_d=250,300,350 and 400 keV. The angular distribution of neutron for E_d=350 keV is shown in Fig. A.1.

From the Table A.2, it is clear that the effect of nonuniformity in tritium distribution is about 0.3 % for incident deuteron energies up to 400 keV.

Appendix 3 Average Reaction Energy

Let P(E)dE denote the probability that D-T reaction occurs in the Ti-T target in energy interval dE,

$$\begin{aligned} P(E)dE &\propto \sigma(x)\phi(x)n_T(x)dx \\ &= \sigma(E)\phi(E)n_T(E)\frac{dx}{dE}dE \\ &\propto \sigma(E)n_T(E)\frac{dx}{dE}dE \\ &\propto (\frac{d\sigma}{d\omega})(E)/(\frac{dE}{dx})(E)\cdot n_T(E)dE \ , \end{aligned} \tag{A.3.1}$$

where $\phi(E)$ is the deutron flux, $\sigma(X)$ the cross section of D-T reaction. In this equation, it is assumed that the deutron flux is constant in the range and the reaction products emitted isotropically in the CM system.

Then,

$$P(E) \propto (\frac{d\sigma}{d\omega})/(\frac{dE}{dx})\cdot n_T(E). \tag{A.3.2}$$

Therefore, the average reaction energy $\langle E \rangle$ is given by

$$\begin{aligned} \langle E \rangle &= \frac{\int_o^{E_d} EP(E)dE}{\int_o^{E_d} P(E)dE} \\ &= \frac{\int_o^{E_d} (\frac{d\sigma}{d\omega})/(\frac{dE}{dx})\cdot n_T(E)\ E\ dE}{\int_o^{E_d} (\frac{d\sigma}{d\omega})/(\frac{dE}{dx})\cdot n_T(E)dE} \end{aligned} \tag{A.3.3}$$

The values of average reaction energy for the ideal tritium profile and for the Model (B) (a=0.8, b=0.6 and E_a=1/2 Ed) are tabulated in Table A.3.

Appendix 4 Differential cross section values for $^{3}He(d,p)^{4}He$ reaction

The cross section values for $^{3}He(d,p)^{4}He$ reaction are tabulated in Table A.4 which is used to obtain the conversion factor from proton to α-particle counts.[3]

Table A.1 The values of $R_\alpha(E_d, \theta_\alpha=179.1°)$, K_{1st} and K_{2nd}

E_d [keV]	R_α	K_{1st}*	K_{2nd}*
200	1.2239	4.647E+07	9.210E+06
205	1.2257	4.653E+07	9.223E+06
210	1.2275	4.660E+07	9.237E+06
215	1.2293	4.667E+07	9.250E+06
220	1.2310	4.673E+07	9.263E+06
225	1.2326	4.680E+07	9.275E+06
230	1.2343	4.686E+07	9.288E+06
235	1.2359	4.692E+07	9.300E+06
240	1.2374	4.698E+07	9.311E+06
245	1.2389	4.703E+07	9.322E+06
250	1.2404	4.709E+07	9.334E+06
255	1.2419	4.715E+07	9.345E+06
260	1.2433	4.720E+07	9.356E+06
265	1.2448	4.726E+07	9.367E+06
270	1.2461	4.731E+07	9.377E+06
275	1.2475	4.736E+07	9.387E+06
280	1.2488	4.741E+07	9.397E+06
285	1.2501	4.746E+07	9.407E+06
290	1.2514	4.751E+07	9.416E+06
295	1.2527	4.756E+07	9.426E+06
300	1.2539	4.760E+07	9.435E+06
305	1.2552	4.765E+07	9.445E+06
310	1.2564	4.770E+07	9.454E+06
315	1.2576	4.774E+07	9.463E+06
320	1.2588	4.779E+07	9.472E+06
325	1.2600	4.784E+07	9.481E+06
330	1.2611	4.788E+07	9.489E+06
335	1.2623	4.792E+07	9.499E+06
340	1.2634	4.796E+07	9.507E+06
345	1.2645	4.801E+07	9.515E+06
350	1.2656	4.805E+07	9.523E+06
355	1.2667	4.809E+07	9.532E+06
360	1.2678	4.813E+07	9.540E+06
365	1.2689	4.817E+07	9.548E+06
370	1.2699	4.821E+07	9.556E+06
375	1.2710	4.825E+07	9.564E+06
380	1.2720	4.829E+07	9.572E+06
385	1.2731	4.833E+07	9.580E+06
390	1.2741	4.837E+07	9.587E+06
395	1.2751	4.841E+07	9.595E+06
400	1.2762	4.845E+07	9.603E+06

* They are used for the first (80° beam lime) and the second (0° beam lime) target rooms.

Table A.2 Angular distribution of D-T neutron, uniform (U) or nonuniform* (NU) loading of tritium

θ_n [deg]	E_d = 250 [keV]			E_d = 300 [keV]		
	U	NU	deviation [%]**	U	NU	deviation [%]
0	1.0555	1.0522	-0.313	1.0579	1.0548	-0.293
10	1.0546	1.0514	-0.303	1.0570	1.0539	-0.293
20	1.0520	1.0489	-0.295	1.0542	1.0513	-0.275
30	1.0477	1.0449	-0.267	1.0497	1.0471	-0.248
40	1.0419	1.0395	-0.230	1.0437	1.0414	-0.220
50	1.0348	1.0328	-0.193	1.0363	1.0344	-0.183
60	1.0267	1.0252	-0.146	1.0278	1.0263	-0.146
70	1.0178	1.0168	-0.098	1.0185	1.0176	-0.088
80	1.0084	1.0080	-0.040	1.0087	1.0083	-0.040
90	0.9988	0.9990	0.014	0.9987	0.9989	0.014
100	0.9894	0.9901	0.069	0.9889	0.9896	0.067
110	0.9804	0.9816	0.121	0.9795	0.9806	0.117
120	0.9720	0.9737	0.170	0.9708	0.9724	0.164
130	0.9645	0.9666	0.214	0.9630	0.9650	0.207
140	0.9581	0.9605	0.253	0.9563	0.9586	0.243
150	0.9530	0.9556	0.282	0.9510	0.9535	0.272
160	0.9492	0.9521	0.304	0.9470	0.9498	0.294
170	0.9469	0.9499	0.315	0.9446	0.9475	0.307
180	0.9461	0.9492	0.322	0.9438	0.9468	0.310

θ_n [deg]	E_d = 350 [keV]			E_d = 400 [keV]		
	U	NU	deviation [%]	U	NU	deviation [%]
0	1.0601	1.0570	-0.292	1.0622	1.0589	-0.311
10	1.0591	1.0561	-0.283	1.0612	1.0580	-0.302
20	1.0563	1.0533	-0.284	1.0582	1.0552	-0.284
30	1.0516	1.0489	-0.257	1.0533	1.0506	-0.256
40	1.0453	1.0430	-0.220	1.0468	1.0444	-0.229
50	1.0376	1.0357	-0.183	1.0388	1.0369	-0.183
60	1.0288	1.0273	-0.146	1.0297	1.0282	-0.146
70	1.0191	1.0182	-0.088	1.0197	1.0188	-0.088
80	1.0090	1.0086	-0.040	1.0092	1.0088	-0.040
90	0.9986	0.9988	0.016	0.9985	0.9987	0.017
100	0.9884	0.9891	0.068	0.9880	0.9887	0.071
110	0.9787	0.9798	0.119	0.9779	0.9791	0.123
120	0.9696	0.9712	0.165	0.9686	0.9703	0.171
130	0.9616	0.9636	0.208	0.9603	0.9623	0.215
140	0.9547	0.9570	0.244	0.9532	0.9556	0.251
150	0.9492	0.9517	0.273	0.9475	0.9501	0.281
160	0.9451	0.9479	0.295	0.9433	0.9461	0.302
170	0.9426	0.9455	0.308	0.9407	0.9437	0.316
180	0.9418	0.9447	0.312	0.9399	0.9429	0.320

* Model (B) (a=0.8, b=0.6, E_a=1/2 Ed)

** (U-NU)/U × 100

Table A.3 Average reaction energy

E_d [keV]	$\langle E \rangle_0$ *1	$\langle E \rangle_1$ *2	deviation [%] *3
150	101.63	88.36	-13.053
155	103.72	90.20	-13.031
160	105.74	92.35	-12.660
165	107.71	94.11	-12.626
170	109.63	96.15	-12.295
175	111.49	97.84	-12.246
180	113.29	99.77	-11.930
185	115.06	101.40	-11.872
190	116.77	103.24	-11.587
195	118.46	104.81	-11.523
200	120.13	106.55	-11.304
205	121.76	108.08	-11.235
210	123.34	109.74	-11.026
215	124.91	111.22	-10.960
220	126.45	112.80	-10.795
225	127.96	114.25	-10.714
230	129.44	115.76	-10.569
235	130.90	117.17	-10.489
240	132.34	118.61	-10.375
245	133.78	119.99	-10.308
250	135.19	121.37	-10.223
255	136.59	122.73	-10.147
260	137.95	124.05	-10.076
265	139.29	125.38	-9.986
270	140.63	126.65	-9.941
275	141.94	127.96	-9.949
280	143.24	129.18	-9.916
285	144.53	130.46	-9.735
290	145.81	131.64	-9.718
295	147.09	132.90	-9.647
300	148.37	134.04	-9.658
305	149.64	135.29	-9.590
310	150.92	136.38	-9.634
315	152.19	137.62	-9.574
320	153.46	138.69	-9.625
325	154.74	139.91	-9.584
330	156.01	140.96	-9.647
335	157.28	142.17	-9.607
340	158.56	143.20	-9.687
345	159.83	144.40	-9.654
350	161.10	145.41	-9.739
355	162.37	146.61	-9.706
360	163.64	147.61	-9.796
365	164.90	148.80	-9.763
370	166.16	149.78	-9.958
375	167.42	150.97	-9.826
380	168.67	151.94	-9.919
385	169.93	153.12	-9.892
390	171.18	154.08	-9.989
395	172.43	155.26	-9.958
400	173.67	156.21	-10.054

*1 Average reaction energy for the ideal tritium profile

*2 Average reaction energy for the Model (B) (a=0.8, b=0.6, E_a=1/2 E_d)

*3 $(\langle E \rangle_0 - \langle E \rangle_1)/\langle E \rangle_0 \times 100$

Table A.4 Differential cross section values for $^{3}He(d,p)^{4}He$ reaction

E_d [keV]	$(\frac{d\sigma}{d\omega},)$ [mb/sr]	E_d [keV]	$(\frac{d\sigma}{d\omega},)$ [mb/sr]
5	2.5	255	387.0
10	5.0	260	404.0
15	7.5	265	420.0
20	10.0	270	436.0
25	12.5	275	453.0
30	15.0	280	469.0
35	17.5	285	485.0
40	20.0	290	501.0
45	22.5	295	518.0
50	25.0	300	534.0
55	29.0	305	549.0
60	33.0	310	563.0
65	37.0	315	581.0
70	41.0	320	598.0
75	46.0	325	611.0
80	50.0	330	624.0
85	54.0	335	635.0
90	58.0	340	646.0
95	62.0	345	653.0
100	66.0	350	659.0
105	73.0	355	665.0
110	80.0	360	670.0
115	86.0	365	675.0
120	93.0	370	679.0
125	100.0	375	683.0
130	106.0	380	686.0
135	112.0	385	687.0
140	119.0	390	688.0
145	125.0	395	687.0
150	131.0	400	685.0
155	141.0	405	686.0
160	151.0	410	686.0
165	161.0	415	685.0
170	171.0	420	683.0
175	182.0	425	678.0
180	192.0	430	673.0
185	202.0	435	670.0
190	212.0	440	668.0
195	222.0	445	664.0
200	232.0	450	659.0
205	246.0	455	654.0
210	260.0	460	649.0
215	274.0	465	644.0
220	288.0	470	639.0
225	302.0	475	636.0
230	315.0	480	632.0
235	329.0	485	629.0
240	343.0	490	624.0
245	357.0	495	615.0
250	371.0	500	605.0

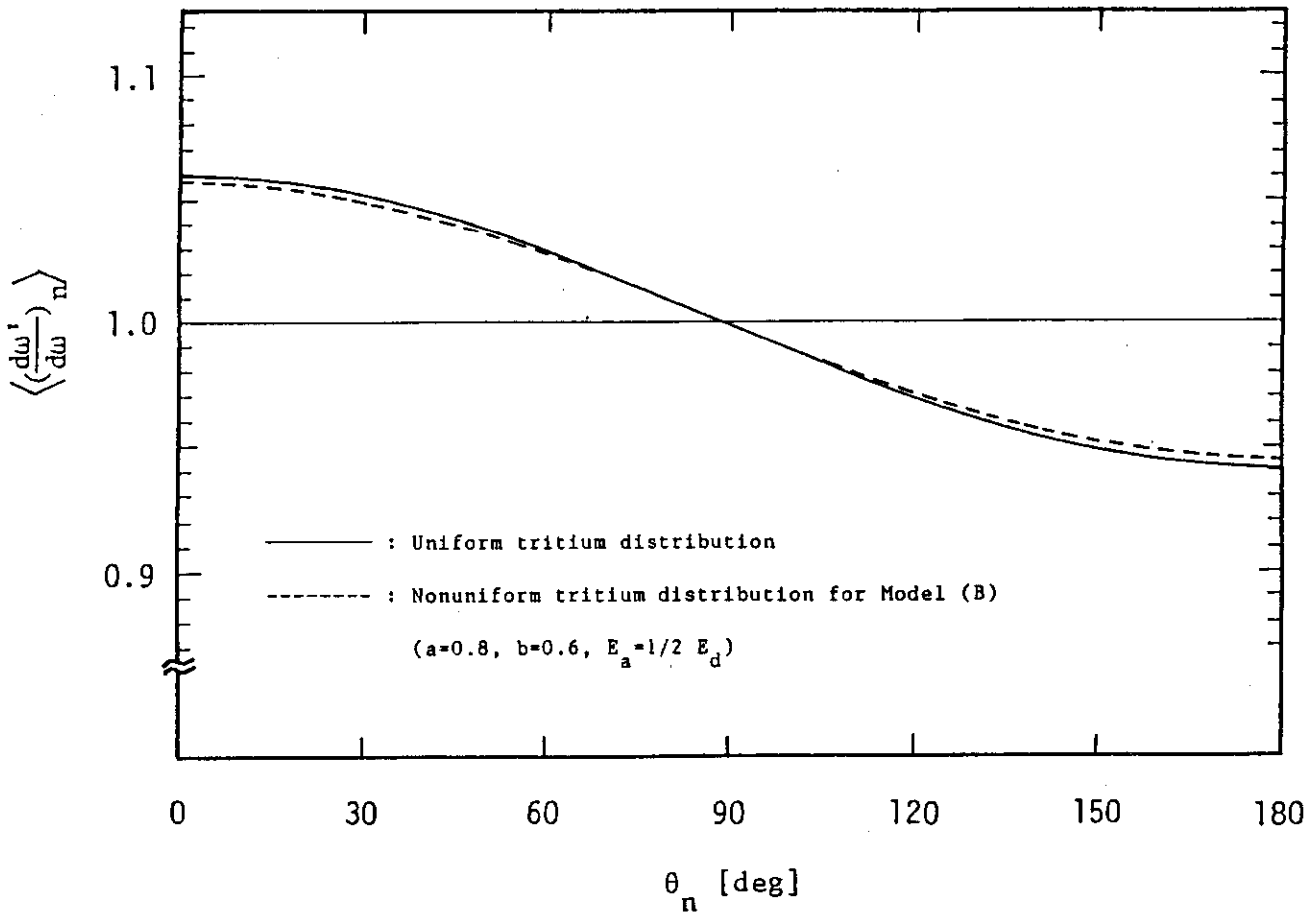

Fig. A.1 Typical angular distribution of D-T neutron (E_d=350 keV)